### Title

Detection and validation of novel mutations in MERTK in a simplex case of retinal degeneration using WGS and hiPSC–RPEs model




### Journal

Human Mutation, 42(2)

### ISSN

1059-7794



### Authors

Biswas, Pooja
Borooah, Shyamanga
Matsui, Hiroko
et al.



### Publication Date

2021-02-01

### DOI

10.1002/humu.24146

Peer reviewed

HHS Public Access

Author manuscript

*Hum Mutat*. Author manuscript; available in PMC 2022 February 01.

Published in final edited form as:

*Hum Mutat*. 2021 February ; 42(2): 189–199. doi:10.1002/humu.24146.

# Detection and validation of novel mutations in *MERTK* in a simplex case of retinal degeneration using WGS and hiPSC-RPEs model

**Pooja Biswas**[1,2], **Shyamanga Borooah**[1], **Hiroko Matsui**[3], **Marina Voronchikhina**[1], **Jason Zhou**[1], **Qais Zawaydeh**[1], **Pongali B Raghavendra**[2,4], **Henry Ferreyra**[1], **S Amer Riazuddin**[5], **Karl Wahlin**[1], **Kelly A Frazer**[3,6], **Radha Ayyagari**[1]

[1]Shiley Eye Institute, University of California San Diego, La Jolla, California, USA.

[2]REVA University, Bengaluru, Karnataka, India.

[3]Institute for Genomic Medicine, University of California, San Diego, La Jolla, California, USA.

[4]School of Regenerative Medicine, Manipal University-MAHE, Bangalore, India.

[5]Wilmer Eye Institute, Johns Hopkins Univesity School of Medicine, Baltimore, Maryland, USA.

[6]Department of Pediatrics, Rady Children's Hospital, Division of Genome Information Sciences, San Diego, California, USA.

## Abstract

Inherited Retinal degenerations (IRD) are a group of genetically heterogeneous conditions with broad clinical phenotypic heterogeneity. A nuclear family of European ancestry with one individual affected by progressive retinal degeneration was analyzed. Whole genome sequencing of the proband and her unaffected sibling identified a novel intron 8 donor splice site variant (c.1296+1G>A) and a novel 731 base pair deletion encompassing exon 9 (Chr2:112751488–112752218) resulting in c.1297_1451del; p.K433_G484fsTer3 in the Mer tyrosine kinase protooncogene (*MERTK*) expressed in retinal pigment epithelium (RPE). The proband carried both variants in the heterozygous state which segregated with disease in the pedigree. These *MERTK* variants are predicted to result in the defective splicing of exon 8 and loss of exon 9 respectively. To evaluate the impact of these novel variants, human induced pluripotent stem cell lines (hiPSC) were reprogrammed from the proband and parental peripheral blood mononuclear cells (PBMCs) and differentiated to hiPSC-RPE. Analysis of the proband's hiPSC-RPE revealed the absence of *MERTK* transcript and protein as well as abnormal phagocytosis when compared

*To whom the correspondence should be addressed: Radha Ayyagari, PhD, 9415 Campus Point Drive, JRC 206, Shiley Eye Institute, University of California San Diego, La Jolla, California, United States, Phone: (858) 534-9029; Fax: (858) 246-0568. rayyagari@ucsd.edu.

CONFLICT OF INTEREST STATEMENT

The authors have no conflict of interest to declare.

WEB RESOURCES

RetNet Database: https://sph.uth.edu/retnet/disease.htm

DATA AVAILABILITY STATEMENT

The metadata and the whole genome sequencing data of the affected individual, II:I and the unaffected sibling, II:II have been deposited in the database of Genotypes and Phenotypes (dbGaP). The public study report page and summary-level phenotype data may be browsed at dbGaP: https://www.ncbi.nlm.nih.gov/projects/gap/cgi-bin/study.cgi?study_id=phs001619.v2.p1.

with the parental hiPSC-RPE. In summary, WGS identified novel compound heterozygous variants in *MERTK* as the underlying cause of IRD in the proband. Further, analysis using an hiPSC-RPE model established a functional impact of novel *MERTK* mutations and revealed the potential mechanism underlying pathology due to these mutations.

## Graphical Abstract

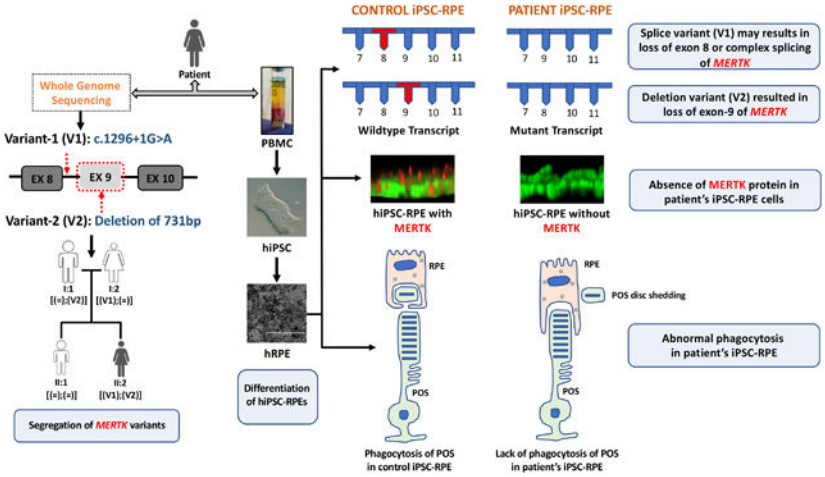


### Keywords

Inherited retinal degenerations (IRDs); Disease modelling; Whole Genome Sequencing; Human iPSC-RPE; RPE Phagocytosis

## INTRODUCTION

Inherited retinal degenerations (IRDs) are a group of genetically heterogeneous conditions that cause irreversible vision loss (Hartong, Berson, & Dryja, 2006; Heckenlively, 1988). IRDs segregate in autosomal dominant, autosomal recessive, X-linked, and mitochondrial patterns of inheritance. There is significant overlap in the clinical phenotypes of these diseases making a diagnosis based on phenotype alone challenging. Several therapeutic approaches are actively being pursued to treat IRDs (DiCarlo, Mahajan, & Tsang, 2018; He, Zhang, & Su, 2015; Rodrigues et al., 2018; Wu et al., 2018). The ability to identify and validate all potential causative variants is critical in directing clinical care that takes advantage of these emerging therapies (Bolz, 2017, 2018; Carss et al., 2017; Corton et al., 2013). Whole genome sequencing (WGS) enables identification of causative variants in non-coding regions, coding regions and large structural changes. However, interpretation of the impact of novel variants in small pedigrees or isolated cases requires experimental validation to establish their causal role in pathology.

In the current study we identified novel, compound heterozygous potentially causative sequence alterations in *MERTK* in a single case with recessive retinitis pigmentosa (RP) using WGS. We have validated the impact of these novel sequence changes on the expression and function of *MERTK* by studying retinal pigment epithelial (RPE) cells

differentiated from the human induced pluripotent stem cells (hiPSCs) generated from the peripheral blood mononuclear cells (PBMCs) of members of the pedigree.

## METHODS

### Patient Information and Ethics Statement:

A pedigree of Scottish/Irish and English/German ancestry with one affected individual, an unaffected brother, and unaffected parents was recruited for the study (Fig-1). All studies were carried out in accordance with the declaration of Helsinki and with the approval of the institutional review board (IRB) of the University of California San Diego.

### Clinical Examination:

The affected individual at age 43, underwent ophthalmic evaluation including fundoscopy, electroretinography (ERG), spectral domain-optical coherence tomography (SD-OCT), and best- corrected visual acuity (BCVA) (Fig-1). In addition, prior medical records of the patient were reviewed. Parents underwent general ophthalmic evaluation including fundoscopy and BCVA.

### Genetic analysis:

Written informed consent was obtained from all participating subjects. Whole blood samples were collected for next generation sequencing (NGS). Genomic DNA extraction was performed using the QIAamp DNA Kit (Qiagen, Germany). Initially, whole exome sequencing (WES) of affected and unaffected siblings was performed using Agilent V5 + UTRs kit (Agilent Technologies, Santa Clara, CA). WGS was performed using Illumina HiSeqX10 (Illumina, San Diego, CA). The reads were mapped using BWA (Li & Durbin, 2009) against the human genome 19 (hg19) and variants were called using GATK as described earlier (Branham et al., 2016; DePristo et al., 2011; Van der Auwera et al., 2013). The annotation was completed using SnpEff (Cingolani et al., 2012), PolyPhen2 (Adzhubei, Jordan, & Sunyaev, 2013) and CADD score (Kircher et al., 2014) and copy number variations (CNVs) were called using GenomeSTRiP (Handsaker et al., 2015) and LUMPY (Layer, Chiang, Quinlan, & Hall, 2014; Li, 2014). Segregation analysis of the candidate variants was carried out using Sanger sequencing (Supp. Table S1).

### Peripheral blood mononuclear cells extraction and cell culture:

Peripheral blood mononuclear cells (PBMCs) from the proband and parents were reprogrammed to hiPSC using CytoTune iPS 2.0 Sendai Reprogramming Kit (ThermoFisher Scientific, Carlsbad, CA) and iPSCs were maintained using standard protocols (Bhise, Wahlin, Zack, & Green, 2013). The passaging of these cells was done using blebbistatin (Sigma-Aldrich, St. Louis, MO) along with mTeSR1 medium and maintained with the fresh mTeSR1 media after 48 hr. The hiPSCs were differentiated to RPE cells (hiPSC-RPE) as described earlier (Bhise et al., 2013; Carr et al., 2009; Lukovic et al., 2015; Vaajasaari et al., 2011). In brief, hiPSCs were grown to confluence and then changed to differentiation media containing 10 mM NIC + 50 nM CTM for two weeks. After 2 weeks, the cells were fed with differentiation media + 10 mM NIC for another 2 weeks. These transformed cells were passaged and cultured for four weeks by daily changing of RPE medium.

### Characterization of hiPSC and hiPSC-RPE cells:

Standard validation of hiPSCs were performed by evaluating the expression of four pluripotency markers using rabbit anti-SOX2 (AB5603, Millipore, Burlington, MA), rabbit anti-OCT4 (ab19857, Abcam, Cambridge, UK), mouse anti-Nanog (ab173368, Abcam, Cambridge, UK) and mouse anti-SSEA4 (FCMAB116P, Millipore, Burlington, MA) antibodies. Standard hiPSCs-RPE characterization was performed by immunostaining for non-specific RPE markers using mouse anti-ZO1 (33–9100, ThermoFisher Scientific, Carlsbad, California), mouse anti-MITF (sc-56726, Santa Cruz Biotechnology Inc., Santa Cruz, California) and rabbit anti-MERTK (ab52968, Abcam, Cambridge, UK), and for a specific RPE marker BEST1 using mouse anti-Bestrophin-1 (NB300–164, Novus Biologicals, Centennial, CO) (Carr et al., 2009; Lukovic et al., 2015; Vaajasaari et al., 2011). Donkey anti-mouse Alexa-488 (ThermoFisher Scientific, Carlsbad, CA), donkey anti-rabbit Alexa-555 (ThermoFisher Scientific, Carlsbad, CA), and donkey anti-mouse Alexa-555 (ThermoFisher Scientific, Carlsbad, CA) were used as secondary antibodies. Images of stained cells were captured using a Nikon A1R confocal microscope (Nikon, Tokyo, Japan). Trans-epithelial resistance (TER) of mature hiPSCs-RPE cells was measured using the Epithelial Volt/Ohm (TEER) Meter 0–10 KΩ Resistance Range with STX2 (EVOM2) as described previously (Gamal et al., 2015).

### Relative expression of *MERTK* transcript in hiPSC-RPEs:

cDNA generated using iScript™ cDNA Synthesis Kit (Bio-Rad, CA) from RNA isolated using RNeasy Mini Kit (Qiagen, Germany) from proband's and parents hiPSC-RPE was used as the template for amplification and sequencing to verify the predicted alterations of exon 8 and 9 sequences in the *MERTK* transcript. Relative expression of total and mutant *MERTK* transcripts was studied using quantitative real time PCR (qRT-PCR). One set of RT Primers (F3 and R3) was designed to amplify a region upstream to the mutations to detect total (wildtype and mutant) *MERTK* transcripts. The second set of RT primers (F4 and R4) was designed (Fig-5A) (Supp. Table S1) to selectively amplify the mutant transcript resulting from the exon 9 deletion of *MERTK* (Supp. Table S1) present in the patient (II:II) and the father (I:I). Another set of primers (F5 and R5) (Fig-5A) (Supp. Table S1) were used to evaluate the possible outcomes of the exon 8 donor splice site mutation in the mother (I:II) and proband (II:II). The findings were compared to those from the unaffected parents. The housekeeping genes *ACTB* and *GAPDH* were used as control reference gene. All analyses were performed in triplicates and mean Ct values were to calculated. The standard deviations for each mean Ct value was calculated for ΔΔCt calculation as described earlier (Mandal et al., 2006). Statistical analysis was performed using Student's t test. The P value <0.0001, which was represented as ***, was considered to be statistically significant.

### Expression of MERTK protein in hiPSC-RPE

**Western blot analysis:** The expression of MERTK protein was examined in the proband, parental and normal control hiPSC and hiPSC-RPE by western blot analysis using an anti-MERTK antibody (Ab52968, Abcam, Cambridge, UK). ACTB was used as loading control.

**Phagocytosis assay:** MERTK plays an important role in phagocytosis of photoreceptor outer segments (Lukovic et al., 2015). Phagocytosis in hiPSC-RPE was studied using a slightly modified version of the assay previously described (Mao & Finnemann, 2013). Bovine retinal photoreceptor rod outer segments (POS) (InVision Bioresources, Seattle, USA) were labeled with FITC isomer I (Invitrogen Corporation, Carlsbad, CA) (Singh et al., 2013). FITC-labeled POS were seeded onto the mature hiPSC-RPE monolayers grown on Matrigel™ Matrix at $1\times10^7$ POS/ml and incubated. In order to detect the internalized POS, the cells were stained with trypan blue, washed with phosphate buffer saline (PBS) and fixed in paraformaldehyde (PFA). Subsequently, the cells were stained with DAPI and Phalloidin; images were captured using Nikon A1RStorm confocal microscope (Nikon, Tokyo, Japan). The number of intracellular FITC labeled POS in hiPSC-RPE were counted using ImageJ 1.52a software. The difference between patient and control groups was evaluated with student's t test.

## RESULTS

### Clinical analysis

The proband, a 43 year old female (Fig-1. II:II), reported night blindness from late in the first decade of life and was first diagnosed with retinal degeneration at age 13 years. She had no significant history of systemic disease or medication intake. She underwent detailed ophthalmic evaluation at age 20 and BCVA was reported to be 20/200 bilaterally. At the time, her Goldmann visual field testing was reported to be full to a large target (V4e) but limited to only 10–20 degrees around central fixation with a small (I-4e) target. Electroretinography (ERG) at the time, reported scotopic visual fields with severely reduced a and b wave amplitudes and photopic ERGs were reduced in amplitude and delayed in timing. Re-examination at 43 years of age revealed that her vision had diminished to the detection of hand motion. Examination revealed bilateral pigmentary changes throughout the retina with mild asymmetry in macular atrophy that was slightly greater on the right than the left (Fig-2 A1 and A3). SD-OCT imaging demonstrated bilateral loss of the ellipsoid zone on SD-OCT (Fig-2 A2 and Fig-2 A4), which suggested a profound loss of retinal photoreceptors. The full-field ERG responses (Fig-2B) were undetectable to all stimuli following the International Society for Clinical Electrophysiology standards for ERG testing in the affected individual at 43 years, while the unaffected control individual exhibited normal rod and cone responses. In summary, the clinical findings for the patient indicated early-onset progressive retinal degeneration.

The patient reported no family history of IRD. The father of the proband was examined in his 80s and had no visual symptoms. During the examination he was bilaterally pseudophakic and had a normal retinal examination with a vision of 20/25 OD and 20/40 OS. Similarly, the mother, of the patient, 80 years old, reported no visual symptoms. During the examination she had a vision of 20/25 OD and 20/35 OS, was bilaterally pseudophakic, and was noted only to have mild age- related maculopathy bilaterally.

## Genetic analysis

**WES and WGS Sequencing and analysis of variants—**WES of the patient's DNA (II:II) did not detect any potential causative variants segregating with the recessive disease but identified four rare heterozygous variants predicted to be damaging in known IRD genes *USH2A, IFT140, MERTK* and *RHO*. While the first three genes are implicated in recessive disease, the fourth one is involved in both dominant and recessive IRD (Table 1).

Whole genome sequencing (WGS) identified approximately 3 million variants in the proband. Filtering these variants as described previously (Chekuri et al., 2018) confirmed the presence of a novel heterozygous splice-site variant, c.1296+1G>A (NC_000002.11:g.112740571G>A) in *MERTK*, which was previously identified by WES analysis (Table 1). In addition, an additional novel heterozygous 731bp deletion (Chr2: 112751488–112752218) that is predicted to result in an out-of-frame deletion of exon 9 in *MERTK* was observed (Fig-3).

Further analysis of rare (<0.0001) variants detected by WGS did not identify any rare variants that can be considered as potential causative mutations either in the coding region or the non-coding region of the *IFT140* or *USH2A* genes.

**Validation of the presence of potential causative variants and segregation analysis—**To verify the presence of the c.1296+1G>A and c.1297_1451del variants in *MERTK*, we designed a set of primers flanking the sequence alterations for PCR and sequencing (Supp. Table S1) (Fig-3A). The presence of c.1296+1G>A in I-II and II-II was verified PCR using F1 and R1 primers (Supp. Table S1) followed by Sanger sequencing (data not shown). Amplification of genomic DNA with F2 and R2 will produce a 947 bp PCR product without the deletion and a 216 bp PCR product in the presence of the deletion. Analysis with these primers detected the 947 bp and 216 bp bands in I:I and II:II, whereas only the 947 bp PCR product was observed in I:II and II:I (Fig-3B). Agarose gel purification followed by Sanger sequencing of the shorter 216 bp PCR product confirmed the loss of 731 bp encompassing exon 9 (Fig-3B & C). Further examination of the sequence flanking the deletion showed the presence of paralogous repeat sequences (GGTGG) on either side of deletion (Fig-3C). Both novel heterozygous variants detected in *MERTK* segregated with disease in the study pedigree (Fig-1).

Segregation analysis of the novel heterozygous p.Arg147Cys variant in *RHO*, a gene implicated in both dominant and recessive retinitis pigmentosa (RP), revealed the presence of this variant in the heterozygous state in the unaffected mother while it was absent in father and unaffected brother of the proband.

**HiPSC and hiPSC-RPE characterization—**The pluripotency of hiPSC lines from the proband (II:II) and unaffected parents (I:I and I:II) was confirmed using OCT4, Nanog, SSEA4 and SOX2 pluripotency markers (Fig-4 panel A to F). The RPE characteristic markers ZO1, MiTF and BEST markers were noted in hiPSC-RPE (Fig-4 panel G to I and Supp. Fig-S1). The TER measurement in the cultured proband and normal control hiPSC-RPE revealed a TER of approximately 200 Ω.cm2 in both samples, which is within the range expected for normal human RPE (150 to 200 Ω.cm2) (Lukovic et al., 2015).

**Expression of *MERTK* transcript in hiPSC-RPE—**The donor splice site variant and deletion variant observed in the proband is predicted to result in aberrant splicing at exon 8 and absence of exon 9 respectively. To validate these mutations, the cDNA synthesized using RNA isolated from hiPSC derived RPE cells was amplified and sequenced (Fig-5A and primers F3, R3, F4, R4, F5 and R5 described in Supp. Table S1).

Analysis for the presence of *MERTK* transcript without exon 9 in the proband and the father (I:I) was performed (Fig-5 B1). The wildtype *MERTK* transcript with exon 9 was present in the unaffected father but absent in the proband (Fig-5 B2). The cDNA sequence of the mutant allele confirmed the absence of exon 9 sequence in both the father (I:I) and proband (II:II) (Fig-3 C).

Analysis of the expression of the *MERTK* transcripts by qRT-PCR using primers (F4 and R4) (Supp. Table S1) that selectively amplify the mutant transcript without exon 9 detected significantly higher levels of transcript in the proband hiPSC-RPE compared with the levels in the father's hiPSC-RPE heterozygous for the *MERTK* deletion variant (Fig-5 B3). While these findings demonstrate the presence of *MERTK* transcript without exon 9 in both I:I and II:II, the data also suggest that a disproportionate instability of the mutant transcripts (e.g. V1 >V2 >> WT in instability) is possibly contributing to the discrepancy in V2 expression.

The levels of total *MERTK* transcript measured by qRT-PCR using primers F3 and R3 that amplify both the wild type and mutant transcripts revealed significantly lower levels of expression of total *MERTK* ($p=0.0003$) in proband hiPSC-RPE compared to parental hiPSC-RPE and normal control hiPSC-RPE (Fig-5 C). These data support the greater instability of the mutant *MERTK* transcripts relative to wildtype transcript.

The donor splice site variant observed in proband and mother could result in the skipping of exon 8 or more complex splicing changes, i.e. for example due to usage of a cryptic splice site. To examine the possible outcomes of the intron 8 donor splice site mutation, amplification of exons 6–10 using cDNA of the mother (I:II) and proband (II:II) with primers F5 and R5 was performed but did not detect the presence of the mutant transcript despite multiple attempts (data not shown). Failure to generate a PCR product could have been due to undetectable levels of the mutant transcript due to nonsense-mediated decay (NMD) or the inclusion of significantly large intronic sequence.

**Expression of MERTK protein in hiPSC-RPE:** Immunostaining of the hiPSC-RPE using antibodies raised against the 1–100 N-terminal amino acids of MERTK demonstrated the absence of MERTK protein in proband, II:II hiPSC-RPE (Fig-6 A1) whereas the MERTK signal localized to the apical side of polarized hiPSC RPE was observed in the control sample (Fig-6 A2). Similarly, western blot analysis of hiPSC and hiPSC-RPE lysate did not detect the presence of a band corresponding to wildtype MERTK (180 KD) (Fig-6 B and 6C) in the proband but did detect a band in the parental samples and an unaffected control. The mutant transcript without exon 9 is predicted to generate a protein of 434 amino acids with wildtype amino acid sequence between 1 to 432 amino acids (exons 1–8) and two additional in frame amino acids before premature termination (about 50kD). Since we were unable to determine the outcome of the intron 8 splice site variant by cDNA analysis, we

were unable to predict a size for the splice site mutant protein. Nevertheless, consistent with the immunocytochemistry data, Western blot analysis detected neither the deletion or splice site mutant MERTK proteins in the proband or parental samples (Fig-6 B and 6C). The absence or low abundance beyond the detection threshold of mutant protein reflects the low level of mutant transcript (Fig-5C). These findings demonstrate the loss of MERTK protein in patient hiPSC-RPE.

**Phagocytosis assay in absence of MERTK in hiPSC-RPEs:** MERTK is known for its important role in phagocytosis of photoreceptor outer segments (POS). To test the impact of *MERTK* mutations detected in the proband on RPE phagocytosis, hiPSC-RPE cells were fed FITC labeled POS. This analysis showed clear engulfment of FITC labeled POS by normal control hiPSC-RPE (Fig-6 D i & iii). Intracellular FITC labeled POS were detected either at minimal or negligible levels in patient hiPSC-RPE (Fig-6 D ii & iv). Quantification of the FITC signal in hiPSC-RPE showed a significantly reduced level of signal in proband hiPSC-RPE compared to control hiPSC-RPE (Fig-6F). These findings demonstrate a functional impact of the compound heterozygous *MERTK* mutations on RPE phagocytosis.

## DISCUSSION

Whole genome analysis of a pedigree with a single affected member with early-onset retinal degeneration identified novel compound heterozygous variants including a donor splice site variant in intron 8 and a large deletion encompassing exon 9 of *MERTK* as the potential underlying cause of retinal degeneration. Besides these, a novel potentially pathogenic heterozygous missense variant c.439C>T, p.Arg147Cys in *Rhodopsin* was also detected. The impact of both *MERTK* variants and the *Rhodopsin* gene variant were unknown which propelled the need for further studies to determine the underlying cause of pathology in this patient.

Mutations in *Rhodopsin* and *MERTK* are both known to lead to IRD in patients and animal models (Dryja, Berson, Rao, & Oprian, 1993; Kijas et al., 2002; Lukovic et al., 2015; Rosenfeld et al., 1992; Vollrath et al., 2001). The proband in this study developed early-onset retinal degeneration within the rod-cone dystrophy spectrum in the first decade with severely diminished ERG response by age 20 (Charbel Issa et al., 2009; Mackay et al., 2010). This was accompanied by early-onset nyctalopia and reduced peripheral and central vision, consistent with retinitis pigmentosa (RP), a *MERTK* associated retinopathy (Shahzadi et al., 2010). Further, the macular atrophy phenotype observed in the proband is unusual for RP, however, it has been noted in a few patients with *MERTK* mutations (Mackay et al., 2010; McHenry et al., 2004). Contrary to the findings in the proband, patients with autosomal dominant *Rhodopsin* associated retinopathy commonly present with disease onset in their second to fourth decades (Andreasson, Ehinger, Abrahamson, & Fex, 1992; Daiger et al., 2014; Rosenfeld et al., 1992; Sung, Davenport, & Nathans, 1993) and can present as a classical RP with bone spicules throughout the retina but may also present with sectoral RP (Berson, Rosner, Weigel-DiFranco, Dryja, & Sandberg, 2002). A rod-cone pattern is usually seen on ERG. The clinical phenotype in our case, the time course of disease onset and progression, and the macular changes were most consistent with a *MERTK* associated retinopathy.

Heterozygous mutations in *Rhodopsin* are involved in causing dominant RP in a large number of patients (Dryja et al., 1993; Kijas et al., 2002). Segregation analysis of the heterozygous *Rhodopsin* variant c.439C>T revealed its presence in the unaffected mother with no retinal abnormalities at the age of 80. No family history of retinal dystrophy was noted particularly on mother's side. In the gnomAD database, this *Rho* variant was listed in the heterozygous state in 56 unrelated individuals (MAF-0.00039) and one subject is homozygous for this variant. The absence of retinal abnormalities in the unaffected mother of the proband and the presence of this variant in 57 individuals listed in the gnomeAD database suggest a possible lack of association between the heterozygous c.439C>T *Rhodopsin* variant and the clinical phenotype of the proband.

*MERTK*, with potential causative mutations detected in the proband, is implicated in the pathology of autosomal recessive retinitis pigmentosa (RP) (Brea-Fernandez et al., 2008). Deletions from a few base pairs to 91 kb in *MERTK* have been reported in other patients with RP, providing further support for the involvement of MERTK in the retinal pathology observed in the proband (Evans et al., 2017; Liu et al., 2019; Ostergaard, Duno, Batbayli, Vilhelmsen, & Rosenberg, 2011; Tschernutter et al., 2006). *MERTK*, expressed in the RPE, plays a critical role in phagocytosis (Audo et al., 2018; Shelby et al., 2015) and in maintaining outer retinal homeostasis. Abnormal RPE phagocytosis results in a buildup of undigested POS leading to photoreceptor cell death and loss of vision (Audo et al., 2018; Lukovic et al., 2015).

The c.1297_1451del variant and the intron 8 donor splice site variant (c.1296+1G>A) in *MERTK* identified in the proband are predicted to result in loss of exon 9 and aberrant splicing of exon 8, respectively. The iPSC-RPE of the proband and parents with the splice site and deletion variants did not affect the viability or morphology in the dish, but our study demonstrate that these mutations cause a loss of MERTK protein and reduction in phagocytosis suggesting that in vivo these mutations impact the phagocytosis of photoreceptor outer segments by RPE leading to retinal degeneration.

Multiple approaches to treat retinal pathology due to mutations in *MERTK* have been reported. The Royal College of Surgeons (RCS) rat with *Mertk* mutation is a good model for *MERTK* associated retinopathy with loss of photoreceptors and abnormal RPE phagocytosis (D'Cruz et al., 2000; Vollrath et al., 2001). Sub-retinal injection of a recombinant replication-deficient adenovirus-encoding rat *Mertk* is observed to restore vision in this rat model (Vollrath et al., 2001). Additional approaches to treat *MERTK* associated retinal degeneration have also been reported to be potentially effective (Lorach et al., 2019). Recently, gene therapy to treat *RPE65* associated retinal dystrophy has been approved by the FDA (Dias et al., 2018). Clinical trials for several other gene-based therapies for IRD are underway (Apte, 2018; Nidetz et al., 2020). Given these advances, identification of causative variants and determination of the impact of novel *MERTK* variants detected in the proband of this pedigree is of high significance for molecular diagnosis, family member counseling and facilitating medical decision making. Furthermore, patient-specific iPSC-RPE will serve as a valuable model system to evaluate therapeutic strategies.

## Supplementary Material

Refer to Web version on PubMed Central for supplementary material.

## ACKNOWLEDGMENTS

We would like to thank all subjects for their participation in this research study; Funding is provided by The Foundation Fighting Blindness, Research to Prevent Blindness, NIH-EY21237, P30-EY22589, NIH-T32CA067754, NIH-EY030591 and Foundation Fighting Blindness.

**Grants:** The Foundation Fighting Blindness, Research to Prevent Blindness, BrightFocus Foundation grant, NIH-EY21237, P30-EY22589, T32EY026590, NIH-EY030591

## REFERENCES

Adzhubei I, Jordan DM, & Sunyaev SR (2013). Predicting functional effect of human missense mutations using PolyPhen-2. Curr Protoc Hum Genet, Chapter 7, Unit7 20. doi:10.1002/0471142905.hg0720s76

Andreasson S, Ehinger B, Abrahamson M, & Fex G (1992). A six-generation family with autosomal dominant retinitis pigmentosa and a rhodopsin gene mutation (arginine-135-leucine). Ophthalmic Paediatr Genet, 13(3), 145–153. doi:10.3109/13816819209046483 [PubMed: 1484692]

Apte RS (2018). Gene Therapy for Retinal Degeneration. Cell, 173(1), 5. doi:10.1016/j.cell.2018.03.021 [PubMed: 29570997]

Audo I, Mohand-Said S, Boulanger-Scemama E, Zanlonghi X, Condroyer C, Demontant V, … Zeitz C (2018). MERTK mutation update in inherited retinal diseases. Hum Mutat, 39(7), 887–913. doi:10.1002/humu.23431 [PubMed: 29659094]

Berson EL, Rosner B, Weigel-DiFranco C, Dryja TP, & Sandberg MA (2002). Disease progression in patients with dominant retinitis pigmentosa and rhodopsin mutations. Invest Ophthalmol Vis Sci, 43(9), 3027–3036. Retrieved from https://www.ncbi.nlm.nih.gov/pubmed/12202526 [PubMed: 12202526]

Bhise NS, Wahlin KJ, Zack DJ, & Green JJ (2013). Evaluating the potential of poly(beta-amino ester) nanoparticles for reprogramming human fibroblasts to become induced pluripotent stem cells. Int J Nanomedicine, 8, 4641–4658. doi:10.2147/IJN.S53830 [PubMed: 24348039]

Bolz HJ (2017). [Next-Generation Sequencing: A Quantum Leap in Ophthalmology Research and Diagnostics]. Klin Monbl Augenheilkd, 234(3), 280–288. doi:10.1055/s-0043-103962 [PubMed: 28355658]

Bolz HJ (2018). [Despite Challenges and Pitfalls: How Ophthalmology Benefits from the Use of Next-Generation Sequencing]. Klin Monbl Augenheilkd, 235(3), 258–263. doi:10.1055/s-0043-122076 [PubMed: 29390234]

Branham K, Matsui H, Biswas P, Guru AA, Hicks M, Suk JJ, … Ayyagari R (2016). Establishing the involvement of the novel gene AGBL5 in retinitis pigmentosa by whole genome sequencing. Physiological Genomics, physiolgenomics 00101 02016. doi:10.1152/physiolgenomics.00101.2016

Brea-Fernandez AJ, Pomares E, Brion MJ, Marfany G, Blanco MJ, Sanchez-Salorio M, … Carracedo A (2008). Novel splice donor site mutation in MERTK gene associated with retinitis pigmentosa. Br J Ophthalmol, 92(10), 1419–1423. doi:10.1136/bjo.2008.139204 [PubMed: 18815424]

Carr AJ, Vugler A, Lawrence J, Chen LL, Ahmado A, Chen FK, … Coffey PJ (2009). Molecular characterization and functional analysis of phagocytosis by human embryonic stem cell-derived RPE cells using a novel human retinal assay. Mol Vis, 15, 283–295. Retrieved from https://www.ncbi.nlm.nih.gov/pubmed/19204785 [PubMed: 19204785]

Carss KJ, Arno G, Erwood M, Stephens J, Sanchis-Juan A, Hull S, … Raymond FL (2017). Comprehensive Rare Variant Analysis via Whole-Genome Sequencing to Determine the Molecular Pathology of Inherited Retinal Disease. Am J Hum Genet, 100(1), 75–90. doi:10.1016/j.ajhg.2016.12.003 [PubMed: 28041643]

Charbel Issa P, Bolz HJ, Ebermann I, Domeier E, Holz FG, & Scholl HP (2009). Characterisation of severe rod-cone dystrophy in a consanguineous family with a splice site mutation in the MERTK gene. Br J Ophthalmol, 93(7), 920–925. doi:10.1136/bjo.2008.147397 [PubMed: 19403518]

Chekuri A, Guru AA, Biswas P, Branham K, Borooah S, Soto-Hermida A, … Ayyagari R (2018). IFT88 mutations identified in individuals with non-syndromic recessive retinal degeneration result in abnormal ciliogenesis. Human Genetics, 137(6–7), 447–458. doi:10.1007/s00439-018-1897-9 [PubMed: 29978320]

Cingolani P, Platts A, Wang le L, Coon M, Nguyen T, Wang L, … Ruden DM (2012). A program for annotating and predicting the effects of single nucleotide polymorphisms, SnpEff: SNPs in the genome of Drosophila melanogaster strain w1118; iso-2; iso-3. Fly (Austin), 6(2), 80–92. doi:10.4161/fly.19695 [PubMed: 22728672]

Corton M, Nishiguchi KM, Avila-Fernandez A, Nikopoulos K, Riveiro-Alvarez R, Tatu SD, … Rivolta C (2013). Exome sequencing of index patients with retinal dystrophies as a tool for molecular diagnosis. PLoS One, 8(6), e65574. doi:10.1371/journal.pone.0065574 [PubMed: 23940504]

D'Cruz PM, Yasumura D, Weir J, Matthes MT, Abderrahim H, LaVail MM, & Vollrath D (2000). Mutation of the receptor tyrosine kinase gene Mertk in the retinal dystrophic RCS rat. Hum Mol Genet, 9(4), 645–651. doi:10.1093/hmg/9.4.645 [PubMed: 10699188]

Daiger SP, Bowne SJ, Sullivan LS, Blanton SH, Weinstock GM, Koboldt DC, … Li Y (2014). Application of next-generation sequencing to identify genes and mutations causing autosomal dominant retinitis pigmentosa (adRP). Adv Exp Med Biol, 801, 123–129. doi:10.1007/978-1-4614-3209-8_16 [PubMed: 24664689]

DePristo MA, Banks E, Poplin R, Garimella KV, Maguire JR, Hartl C, … Daly MJ (2011). A framework for variation discovery and genotyping using next-generation DNA sequencing data. Nature Genetics, 43(5), 491–498. doi:10.1038/ng.806 [PubMed: 21478889]

Dias MF, Joo K, Kemp JA, Fialho SL, da Silva Cunha A Jr., Woo SJ, & Kwon YJ (2018). Molecular genetics and emerging therapies for retinitis pigmentosa: Basic research and clinical perspectives. Prog Retin Eye Res, 63, 107–131. doi:10.1016/j.preteyeres.2017.10.004 [PubMed: 29097191]

DiCarlo JE, Mahajan VB, & Tsang SH (2018). Gene therapy and genome surgery in the retina. J Clin Invest, 128(6), 2177–2188. doi:10.1172/JCI120429 [PubMed: 29856367]

Dryja TP, Berson EL, Rao VR, & Oprian DD (1993). Heterozygous missense mutation in the rhodopsin gene as a cause of congenital stationary night blindness. Nat Genet, 4(3), 280–283. doi:10.1038/ng0793-280 [PubMed: 8358437]

Evans DR, Green JS, Johnson GJ, Schwartzentruber J, Majewski J, Beaulieu CL, … Consortium FC (2017). Novel 25 kb Deletion of MERTK Causes Retinitis Pigmentosa With Severe Progression. Invest Ophthalmol Vis Sci, 58(3), 1736–1742. doi:10.1167/iovs.16-20864 [PubMed: 28324114]

Gamal W, Borooah S, Smith S, Underwood I, Srsen V, Chandran S, … Dhillon B (2015). Real-time quantitative monitoring of hiPSC-based model of macular degeneration on Electric Cell-substrate Impedance Sensing microelectrodes. Biosens Bioelectron, 71, 445–455. doi:10.1016/j.bios.2015.04.079 [PubMed: 25950942]

Handsaker RE, Van Doren V, Berman JR, Genovese G, Kashin S, Boettger LM, & McCarroll SA (2015). Large multiallelic copy number variations in humans. Nat Genet, 47(3), 296–303. doi:10.1038/ng.3200 [PubMed: 25621458]

Hartong DT, Berson EL, & Dryja TP (2006). Retinitis pigmentosa. Lancet, 368(9549), 1795–1809. doi:10.1016/S0140-6736(06)69740-7 [PubMed: 17113430]

He Y, Zhang Y, & Su G (2015). Recent advances in treatment of retinitis pigmentosa. Curr Stem Cell Res Ther, 10(3), 258–265. doi:10.2174/1574888×09666141027103552 [PubMed: 25345673]

Heckenlively JR (1988). Retinitis Pigmentosa (1 ed.). Philadelphia: J.B. Lippincott Company.

Kijas JW, Cideciyan AV, Aleman TS, Pianta MJ, Pearce-Kelling SE, Miller BJ, … Acland GM (2002). Naturally occurring rhodopsin mutation in the dog causes retinal dysfunction and degeneration mimicking human dominant retinitis pigmentosa. Proc Natl Acad Sci U S A, 99(9), 6328–6333. doi:10.1073/pnas.082714499 [PubMed: 11972042]

Kircher M, Witten DM, Jain P, O'Roak BJ, Cooper GM, & Shendure J (2014). A general framework for estimating the relative pathogenicity of human genetic variants. Nature Genetics, 46(3), 310–315. doi:10.1038/ng.2892 [PubMed: 24487276]

Layer RM, Chiang C, Quinlan AR, & Hall IM (2014). LUMPY: a probabilistic framework for structural variant discovery. Genome Biol, 15(6), R84. doi:10.1186/gb-2014-15-6-r84 [PubMed: 24970577]

Li H (2014). Toward better understanding of artifacts in variant calling from high-coverage samples. Bioinformatics, 30(20), 2843–2851. doi:10.1093/bioinformatics/btu356 [PubMed: 24974202]

Li H, & Durbin R (2009). Fast and accurate short read alignment with Burrows-Wheeler transform. Bioinformatics, 25(14), 1754–1760. doi:10.1093/bioinformatics/btp324 [PubMed: 19451168]

Liu S, Bi JG, Hu Y, Tang D, Li B, Zhu P, … Dai Y (2019). Targeted next generation sequencing identified novel loss-of-function mutations in MERTK gene in Chinese patients with retinitis pigmentosa. Mol Genet Genomic Med, 7(4), e00577. doi:10.1002/mgg3.577 [PubMed: 30790467]

Lorach H, Kang S, Bhuckory MB, Trouillet A, Dalal R, Marmor M, & Palanker D (2019). Transplantation of Mature Photoreceptors in Rodents With Retinal Degeneration. Transl Vis Sci Technol, 8(3), 30. doi:10.1167/tvst.8.3.30

Lukovic D, Artero Castro A, Delgado AB, Bernal Mde L, Luna Pelaez N, Diez Lloret A, … Bhattacharya SS (2015). Human iPSC derived disease model of MERTK-associated retinitis pigmentosa. Sci Rep, 5, 12910. doi:10.1038/srep12910 [PubMed: 26263531]

Mackay DS, Henderson RH, Sergouniotis PI, Li Z, Moradi P, Holder GE, … Moore AT (2010). Novel mutations in MERTK associated with childhood onset rod-cone dystrophy. Mol Vis, 16, 369–377. Retrieved from https://www.ncbi.nlm.nih.gov/pubmed/20300561 [PubMed: 20300561]

Mandal MN, Vasireddy V, Reddy GB, Wang X, Moroi SE, Pattnaik BR, … Ayyagari R (2006). CTRP5 is a membrane-associated and secretory protein in the RPE and ciliary body and the S163R mutation of CTRP5 impairs its secretion. Investigative Ophthalmology and Visual Science, 47(12), 5505–5513. doi:10.1167/iovs.06-0312 [PubMed: 17122142]

Mao Y, & Finnemann SC (2013). Analysis of photoreceptor outer segment phagocytosis by RPE cells in culture. Methods Mol Biol, 935, 285–295. doi:10.1007/978-1-62703-080-9_20 [PubMed: 23150376]

McHenry CL, Liu Y, Feng W, Nair AR, Feathers KL, Ding X, … Thompson DA (2004). MERTK arginine-844-cysteine in a patient with severe rod-cone dystrophy: loss of mutant protein function in transfected cells. Investigative Ophthalmology and Visual Science, 45(5), 1456–1463. Retrieved from http://www.ncbi.nlm.nih.gov/entrez/query.fcgi?cmd=Retrieve&db=PubMed&dopt=Citation&list_uids=15111602 [PubMed: 15111602]

Nidetz NF, McGee MC, Tse LV, Li C, Cong L, Li Y, & Huang W (2020). Adeno-associated viral vector-mediated immune responses: Understanding barriers to gene delivery. Pharmacol Ther, 207, 107453. doi:10.1016/j.pharmthera.2019.107453 [PubMed: 31836454]

Ostergaard E, Duno M, Batbayli M, Vilhelmsen K, & Rosenberg T (2011). A novel MERTK deletion is a common founder mutation in the Faroe Islands and is responsible for a high proportion of retinitis pigmentosa cases. Molecular Vision, 17, 1485–1492. Retrieved from https://www.ncbi.nlm.nih.gov/pubmed/21677792 [PubMed: 21677792]

Rodrigues GA, Shalaev E, Karami TK, Cunningham J, Slater NKH, & Rivers HM (2018). Pharmaceutical Development of AAV-Based Gene Therapy Products for the Eye. Pharm Res, 36(2), 29. doi:10.1007/s11095-018-2554-7 [PubMed: 30591984]

Rosenfeld PJ, Cowley GS, McGee TL, Sandberg MA, Berson EL, & Dryja TP (1992). A null mutation in the rhodopsin gene causes rod photoreceptor dysfunction and autosomal recessive retinitis pigmentosa. Nature Genetics, 1(3), 209–213. Retrieved from http://www.ncbi.nlm.nih.gov/entrez/query.fcgi?cmd=Retrieve&db=PubMed&dopt=Citation&list_uids=1303237 [PubMed: 1303237]

Shahzadi A, Riazuddin SA, Ali S, Li D, Khan SN, Husnain T, … Riazuddin S (2010). Nonsense mutation in MERTK causes autosomal recessive retinitis pigmentosa in a consanguineous Pakistani family. Br J Ophthalmol, 94(8), 1094–1099. doi:10.1136/bjo.2009.171892 [PubMed: 20538656]

Shelby SJ, Feathers KL, Ganios AM, Jia L, Miller JM, & Thompson DA (2015). MERTK signaling in the retinal pigment epithelium regulates the tyrosine phosphorylation of GDP dissociation inhibitor alpha from the GDI/CHM family of RAB GTPase effectors. Exp Eye Res, 140, 28–40. doi:10.1016/j.exer.2015.08.006 [PubMed: 26283020]

Singh S, Bingol B, Morgenroth A, Mottaghy FM, Moller M, & Schmaljohann J (2013). Radiolabeled nanogels for nuclear molecular imaging. Macromol Rapid Commun, 34(7), 562–567. doi:10.1002/marc.201200744 [PubMed: 23423755]

Sung CH, Davenport CM, & Nathans J (1993). Rhodopsin mutations responsible for autosomal dominant retinitis pigmentosa. Clustering of functional classes along the polypeptide chain. J Biol Chem, 268(35), 26645–26649. Retrieved from https://www.ncbi.nlm.nih.gov/pubmed/8253795 [PubMed: 8253795]

Tschernutter M, Jenkins SA, Waseem NH, Saihan Z, Holder GE, Bird AC, … Webster AR (2006). Clinical characterisation of a family with retinal dystrophy caused by mutation in the Mertk gene. Br J Ophthalmol, 90(6), 718–723. doi:10.1136/bjo.2005.084897 [PubMed: 16714263]

Vaajasaari H, Ilmarinen T, Juuti-Uusitalo K, Rajala K, Onnela N, Narkilahti S, … Skottman H (2011). Toward the defined and xeno-free differentiation of functional human pluripotent stem cell-derived retinal pigment epithelial cells. Mol Vis, 17, 558–575. Retrieved from https://www.ncbi.nlm.nih.gov/pubmed/21364903 [PubMed: 21364903]

Van der Auwera GA, Carneiro MO, Hartl C, Poplin R, Del Angel G, Levy-Moonshine A, … DePristo MA (2013). From FastQ data to high confidence variant calls: the Genome Analysis Toolkit best practices pipeline. Curr Protoc Bioinformatics, 43, 11 10 11–33. doi:10.1002/0471250953.bi1110s43 [PubMed: 25431634]

Vollrath D, Feng W, Duncan JL, Yasumura D, D'Cruz PM, Chappelow A, … LaVail MM (2001). Correction of the retinal dystrophy phenotype of the RCS rat by viral gene transfer of Mertk. Proc Natl Acad Sci U S A, 98(22), 12584–12589. doi:10.1073/pnas.221364198 [PubMed: 11592982]

Wu J, Frady LN, Bash RE, Cohen SM, Schorzman AN, Su YT, … Miller CR (2018). MerTK as a therapeutic target in glioblastoma. Neuro Oncol, 20(1), 92–102. doi:10.1093/neuonc/nox111 [PubMed: 28605477]

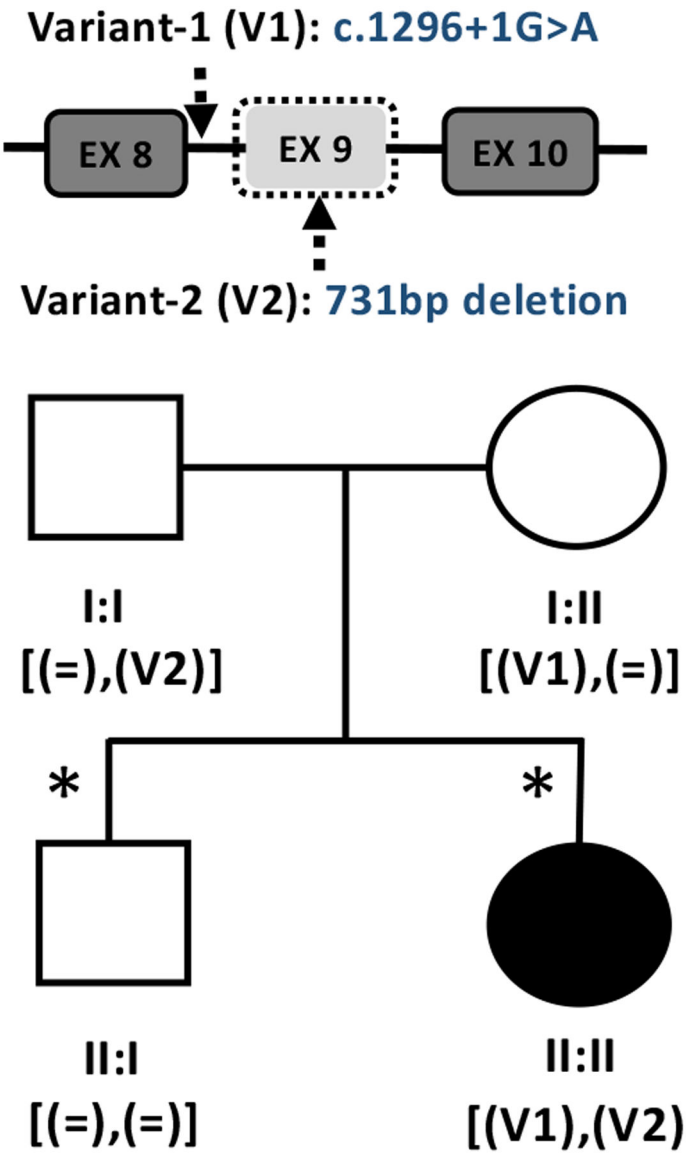


**Fig.1. Segregation of *MERTK* mutations in a pedigree of European ancestry with retinal degeneration.**

Two heterozygous mutations; c.1296+1G>A and Chr2:112751488–112752218 (731bp) deletion in *MERTK*, V1 and V2 respectively, segregated with retinal degeneration in this pedigree. WES and WGS data were obtained from individuals shown with asterisks.

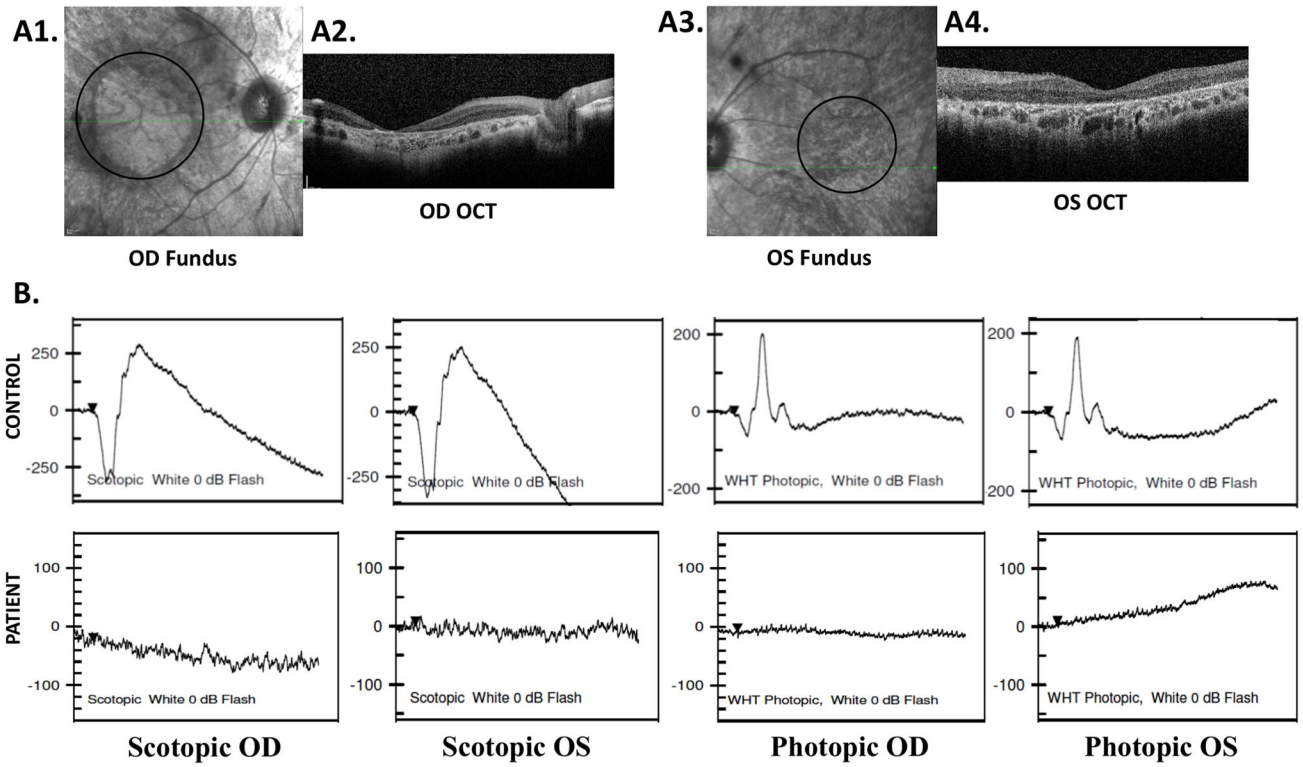


**Fig.2. Near infra-red fundus images and full-field electroretinogram responses in the proband.**

**(A)** Near infrared images and SD-OCT images from the eyes of the affected proband show loss of ellipsoid zone at the age of 43 years and retinal and RPE atrophy. A1-A2 images are from right eye (OD) and A3-A4 images are from the left eye (OS) **(B)** Scotopic and photopic responses at 0db and 30Hz flicker responses of the proband at age 43 years were unrecordable suggestive of severe loss rod and cone photoreceptor response.

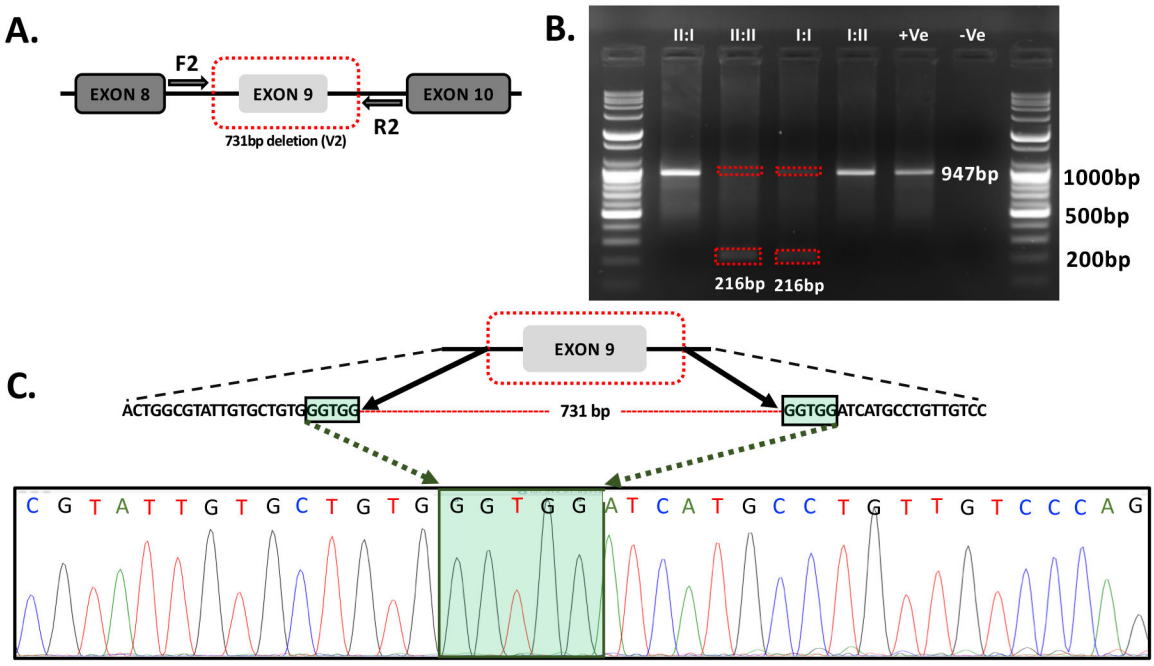


**Fig.3. Validation of 731 bp *MERTK* deletion using gel electrophoresis and Sanger sequencing.**

**(A)** Cartoon showing the genomic region involving the deletion. The 731 bp deletion (spanning part of intron 8, exon 9 and part of intron 9) are shown with a dotted line in red. Forward (F2) and reverse (R2) are the primers used for the amplification of genomic DNA. **(B)** Image of PCR products separated by gel electrophoresis: The presence of 947 bp PCR product in unaffected parents (I:I, I:II) and unaffected sibling (II:I). A 216 bp PCR product was noted in the father (I:I) and the affected individual (II:II). +Ve is the human genomic DNA positive control and -Ve is the negative control without any genomic DNA. **(C)** Schematic showing the deleted region and sequence tracing of the 216 bp PCR product covering the junction fragment and paralogous sequences flanking the deletion. The presence of paralogous repeats GGTGG (highlighted in green) flanking the deleted region is observed.

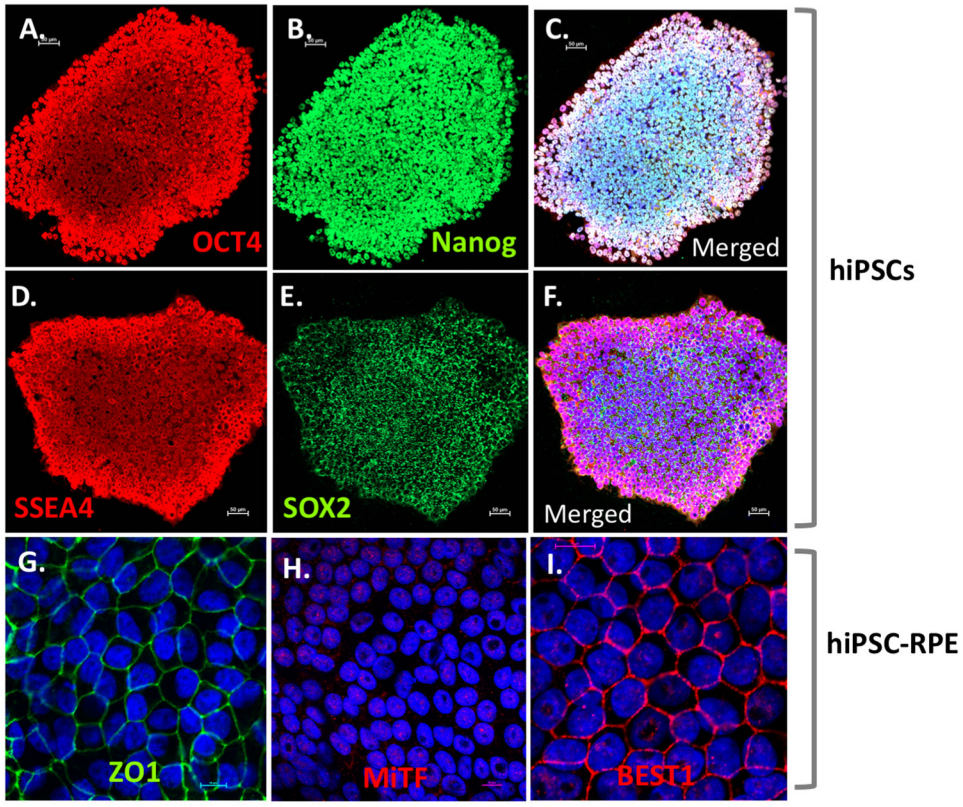


**Fig.4. Characterization of hiPSCs and hiPSC-RPE cells.**

hiPSC lines were stained with (A). OCT4 (red); (B) Nanog (green); (D) SSEA4 (red) and (E) SOX2 (green) antibodies. The merged images of A, B and D, E are shown in C and F respectively. RPE markers (G) ZO1 (green) and (H) the helix-loop-helix leucine zipper transcription factor MiTF (red) and (I) BEST1 localized to the basal side of hiPSC-RPE are shown. All figures are scaled to 50μm.

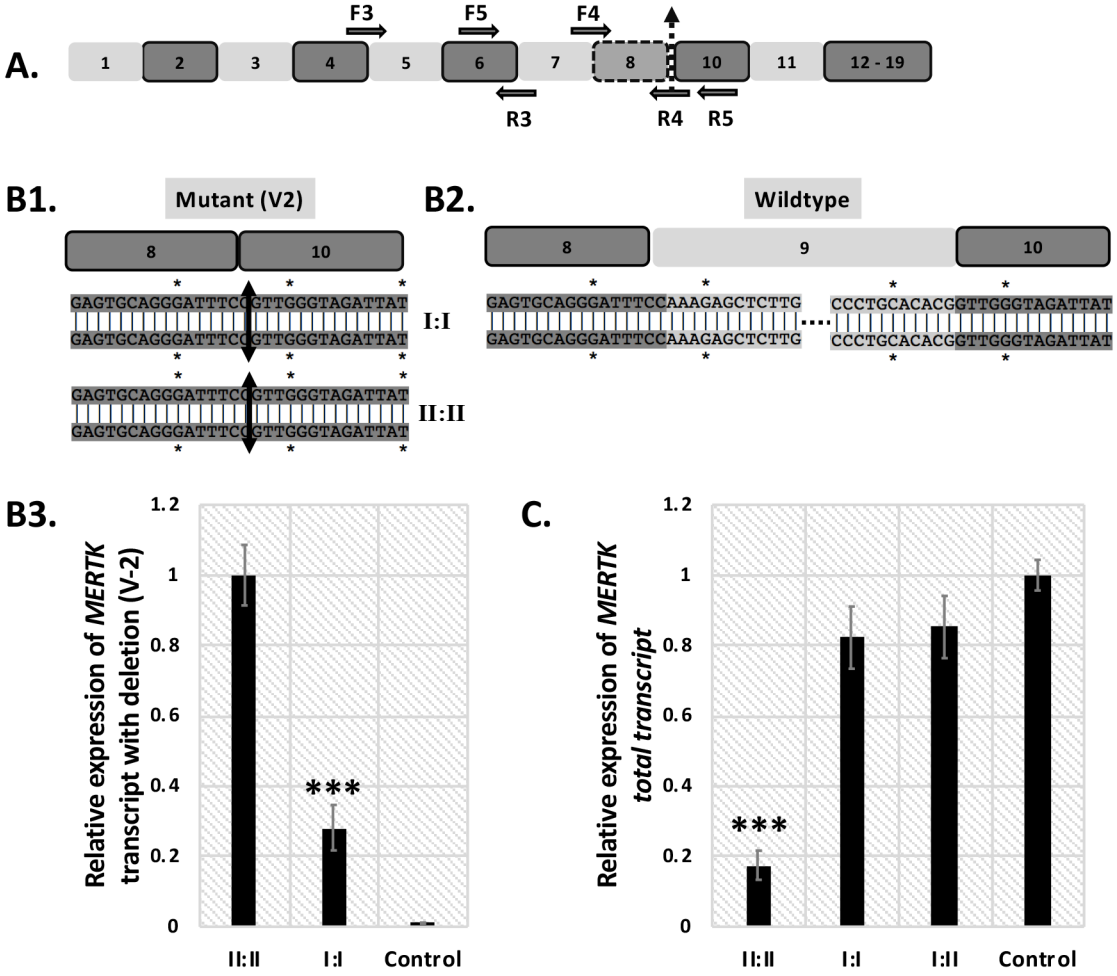


**Fig.5. Expression profile of *MERTK* transcript in hiPSC-RPE.**

**(A)** Cartoon showing the positions of the two mutations in *MERTK* cDNA: aberrant splicing of exon 8 indicated with a dashed line (exons are not to scale) and a deletion of exon 9 indicated by a dotted arrow between exons 8 and 10. F3 and R3 represent the primers used to amplify an upstream region common to both wildtype and mutant transcripts and listed in Table 1. F4 and R4 represent the primers used for RT-PCR to selectively amplify the exon 9 deletion mutant transcript. **(B1)** The sequence of mutant *MERTK* cDNA isolated from the II:II and I:I hiPSC-RPE amplified with primers F4 and R5 showed deletion of exon 9. **(B2)** Sequence of wildtype *MERTK* transcript, including the presence of exon 9 sequence found only in I:I. The dotted line indicates the sequence of exon 9 that is not shown in the figure. **(B3)** Analysis of the relative expression of mutant *MERTK* transcript with the exon 9 deletion is significantly higher (P=0.0003) in the proband (II:II) compared to father (I:I) and control hiPSC-RPE. **(C)** Relative expression of total *MERTK* transcript in the proband hiPSC-RPE was significantly lower (P=0.0003) than in parental hiPSC-RPE and control.

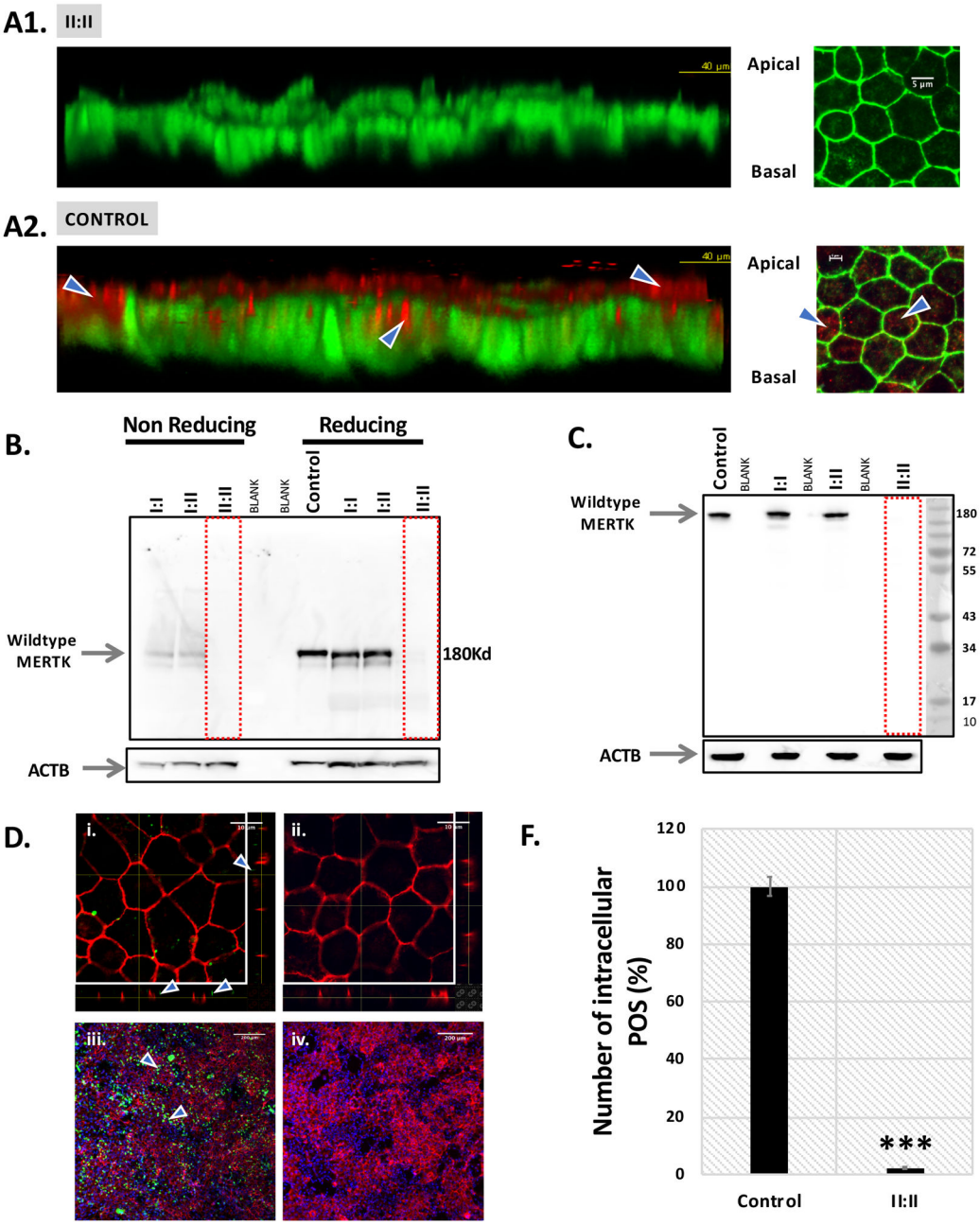


**Fig.6. MERTK protein expression in hiPSCs and hiPSC-RPE cells.**

**(A1)** Immunocytochemistry 3D and 2D images of hiPSC-RPE from the proband (II:II) show that MERTK (red) is not detectable; hiPSC-RPE are labeled with tight junction marker ZO-1 (green). **(A2)** In the control sample, MERTK (red) is localized apically in polarized hiPSC-RPE. ZO1 staining in green is seen in both affected II:II and the control. **(B)** Western blot analysis of lysates of hiPSC. Lanes 1–3: prepared in non-reducing buffer while the lysates loaded in lanes 6–9 are prepared in reducing buffer. The presence of an immunopositive band corresponding to wild type MERTK was detected in I:I and I:II, but not in the proband, II:II under both conditions. **(C)** Western blot analysis of hiPSC-RPE lysates with MERTK antibodies. The presence of wildtype MERTK was detected in I:I and I:II, but not in the

lysate of hiPSC-RPE of the proband. ACTB was used as loading control. **(D)** Fig. i and ii are scaled to 10μm. hiPSC-RPE of (i and iii) control and proband (ii and iv) fed with FITC labeled photoreceptor outer segments (green). Cells were stained with phallodin (red). POS engulfed by hiPSC-RPE (green) are seen in i and iii, whereas these were absent or negligible in ii and iv suggestive of a severe deficiency in phagocytosis. Fig. iii and iv were taken at 20X magnification and scale bar is 200μm. **(F)** The number of intracellular FITC labeled POS was found to be significantly low in hiPSC-RPE of the proband II:I ($P<0.0001$) compared to hiPSC-RPE of the control.

**Table 1:**

Heterozygous variants detected by WES in IRD associated genes.

| Gene | Chr | Position | rsID | REF | ALT | gnomAD | cDNA | Protein | PolyPhen2 |
|---|---|---|---|---|---|---|---|---|---|
| *USH2A* | chr1 | 215802242 | rs111033269 | C | T | 0.003298 | c.15433G>A | p.Val5145Ile | Possibly damaging |
| *IFT140* | chr16 | 1657140 | rs372148301 | A | G | N/A | c.128T>C | p.Val43Ala | Probably damaging |
| *MERTK* | chr2 | 112740571 | rs774577413 | G | A | 0.00003186 | c.1296+1G>A | N/A | N/A |
| *RHO* | chr3 | 129249796 | rs200165530 | C | T | 0.0001732 | c.439C>T | p.Arg147Cys | Probably damaging |

**Abbreviation:** Chr: Chromosome; REF: Reference allele; ALT: Alternative allele; N/A: Not available..